



Ant Colony Pheromone Mechanism-Based Passive Localization Using UAV Swarm

Yongkun Zhou ¹, Dan Song ², Bowen Ding ¹, Bin Rao ¹, Man Su ³ and Wei Wang ^{1,*}

¹ The School of Electronics and Communication Engineering, Sun Yat-sen University, Shenzhen 518000, China; zhoyk6@mail2.sysu.edu.cn (Y.Z.); dingbw@mail2.sysu.edu.cn (B.D.); raob@mail.sysu.edu.cn (B.R.)

² The College of Information and Communication, National University of Defense Technology, Xi'an 710006, China; dansong91@hotmail.com

³ The Beijing Institute of Tracking and Telecommunication Technology, Beijing 100080, China; suman_bcng@163.com

* Correspondence: wangw278@mail.sysu.edu.cn

Abstract: The problem of passive localization using an unmanned aerial vehicle (UAV) swarm is studied. For multi-UAV localization systems with limited communication and observation range, the challenge is how to obtain accurate target state consistency estimates through local UAV communication. In this paper, an ant colony pheromone mechanism-based passive localization method using a UAV swarm is proposed. Different from traditional distributed fusion localization algorithms, the proposed method makes use of local interactions among individuals to process the observation data with UAVs, which greatly reduces the cost of the system. First, the UAVs that have detected the radiation source target estimate the rough target position based on the pseudo-linear estimation (PLE). Then, the ant colony pheromone mechanism is introduced to further improve localization accuracy. The ant colony pheromone mechanism consists of two stages: pheromone injection and pheromone transmission. In the pheromone injection mechanism, each UAV uses the maximum likelihood (ML) algorithm with the current observed target bearing information to correct the initial target position estimate. Then, the UAV swarm weights and fuses the target position information between individuals based on the pheromone transmission mechanism. Numerical results demonstrate that the accuracy of the proposed method is better than that of traditional localization algorithms and close to the Cramer–Rao lower bound (CRLB) for small measurement noise.

Keywords: passive localization; unmanned aerial vehicle (UAV) swarm; ant colony pheromone mechanism



Citation: Zhou, Y.; Song, D.; Ding, B.; Rao, B.; Su, M.; Wang, W. Ant Colony Pheromone Mechanism-Based Passive Localization Using UAV Swarm. *Remote Sens.* **2022**, *14*, 2944. <https://doi.org/10.3390/rs14122944>

Academic Editor: Biswajeet Pradhan

Received: 24 April 2022

Accepted: 15 June 2022

Published: 20 June 2022

Publisher's Note: MDPI stays neutral with regard to jurisdictional claims in published maps and institutional affiliations.



Copyright: © 2022 by the authors. Licensee MDPI, Basel, Switzerland. This article is an open access article distributed under the terms and conditions of the Creative Commons Attribution (CC BY) license (<https://creativecommons.org/licenses/by/4.0/>).

1. Introduction

Passive localization technology using unmanned aerial vehicle (UAV) swarms has been developed and widely used in industry and military fields in recent years [1]. At present, the localization methods of UAV swarms can be mainly divided into two types: active localization and passive localization. Different from active localization, which actively emits electromagnetic waves, passive localization systems only receive and analyze the radiation source signal emitted by targets to obtain their location.

In actual application scenarios, time difference of arrival (TDOA) [2–6], received signal strength (RSS) [7–11], frequency difference of arrival (FDOA) [12], angle of arrival (AOA) [13–22], and their combined algorithms [23–32] are common passive localization techniques. However, TDOA and FDOA localization methods require precise timing and synchronization, which increases the cost and complexity of the implementation. The performance of RSS localization significantly relies on the environment and thus, it is often used in indoor localization scenarios. Since the AOA source localization method does not require synchronization between receivers like TDOA localization, it is widely used [33].

In the application of AOA passive localization, the noise measurement equation is highly nonlinear with respect to the unknown target position. One of the most commonly used algorithms is the pseudo-linear estimator (PLE), which concentrates the nonlinear term into a noise term and estimates the target position using the least-square (LS) optimization algorithm [13,14]. By calculating the PL equation error, a distance weighted least-squares (DWLS) algorithm can be developed to more precisely measure the target position [15]. Meanwhile, how to reduce the estimation bias in AOA localization becomes an important problem. The maximum likelihood estimator (MLE) can be used to eliminate the measurement error of the system [16–18]. In terms of passive localization research for UAVs, the paired AOA information is used to improve the localization performance of the system [19]. The theory of UAV optimal heading angle generation is described in [20]. In some complex urban environments, the UAV passive localization is affected by the occlusion of buildings. The AOA localization algorithm for multipath fading and non-line-of-sight (NLOS) propagation is researched in [21]. The statistical algorithms are applied in [22] to find optimal and sub-optimal estimates. However, due to the limitations of UAVs' computing power and real-time transmission bandwidth, the observed data of the above algorithms usually need to be transmitted to a ground center for processing. The main disadvantages of the centralized localization methods can be divided into the following: (a) too much dependence on the fusion center. If the link is cut off or interfered, the overall localization performance will be degraded; (b) localization algorithms cannot respond quickly to the emerging radiation source.

Meanwhile, some progress has been made in the research on decentralized mobile node localization. A mobile wireless sensor network localization algorithm was proposed in [34], which improved the localization accuracy by using the Monte Carlo method. Ref. [35] introduced a delay-tolerant algorithm that eliminates the processing constraints of static sensor nodes. For the self-organizing network, Ref. [36] researched the cooperative method of network localization and node tracking, which improved the tracking performance of the system. The method mentioned above is realized on the premise that all sensor network nodes can receive the target signal. However, the beamwidth of UAV reconnaissance antennae is usually narrow in practical scenarios, and only a few UAVs can receive the target signal first. In this paper, the above problems can be solved by the ant colony localization algorithm based on the biological self-organization effect.

The ant colony pheromone mechanism originates from observing the self-organizing behavior of real ants to explore the cooperation mechanism [37]. Information transferring between individuals and the environment depends on the pheromone production [38]. Inspired by the ant colony foraging, this paper proposes a passive localization algorithm for UAV swarms based on the ant colony pheromone mechanism. Without increasing the number of UAVs, the target position can be accurately estimated.

Compared with existing methods, the main contributions of this paper are summarized as follows.

(a) Under the condition of limited UAV communication and observation range, the proposed method can obtain accurate target state consistency estimation through local UAV communication. Target position can be estimated by using only the information interaction between individuals. (b) The ant colony pheromone mechanism is introduced into the UAV swarm passive localization scenario to improve localization accuracy. (c) The influence of different passive localization algorithms and relevant parameters, e.g., the number of UAVs, the communication radius of UAV, on localization accuracy, are analyzed.

The rest of this paper is organized as follows: Section 2 models the scenario of passive localization of a UAV swarm. Section 3 contains a detailed analysis of the passive location algorithm based on the ant colony pheromone mechanism proposed in this paper. In Section 4, the performances of different algorithms are analyzed to demonstrate the effectiveness of the proposed method. Concluding remarks are given in Section 5.

2. Problem Description and Modeling

The UAV swarm passive localization geometry is shown in Figure 1. In order to obtain better localization result, it is assumed that K UAVs are evenly distributed in the rectangular area,

$$(x_i, y_i) \in [x_{min}, x_{max}] \times [y_{min}, y_{max}]. \quad (1)$$

Assume that each UAV can only communicate with UAVs within a certain distance and denote this communication distance as r_c . The basic condition of short-range communication between the i th UAV and the j th UAV can be written as:

$$r_{i,j} = \sqrt{(x_i - x_j)^2 + (y_i - y_j)^2}, r_{i,j} \leq r_c, (\forall i \neq j). \quad (2)$$

The position matrix of the UAV swarm can be expressed as:

$$\mathbf{U} = [\mathbf{u}_1, \mathbf{u}_2, \dots, \mathbf{u}_K]^T, \mathbf{u}_k = [x_k, y_k]^T, k = 1, 2, \dots, K \quad (3)$$

where u_k denotes the position vector of the UAV; x_k and y_k represent the coordinate information. Let $\mathbf{p} = [x, y]^T$ denote the position of a radiation source target. The angle between UAV and the target θ_k can be calculated by [39]:

$$\sin \theta_k = \frac{x - x_k}{r_k}, \cos \theta_k = \frac{y - y_k}{r_k} \quad (4)$$

where $r_k = \|\mathbf{p} - \mathbf{u}_k\|$ is the distance between the UAV and the target.

The position relationship between UAVs is determined by

$$\sin \theta_{i,j} = \frac{x_i - x_j}{r_{i,j}}, \cos \theta_{i,j} = \frac{y_i - y_j}{r_{i,j}} \quad (5)$$

where $\theta_{i,j}$ denotes the angle between the i th UAV and the j th UAV; (x_i, y_i) and (x_j, y_j) represent the coordinate information of u_i and u_j , respectively.

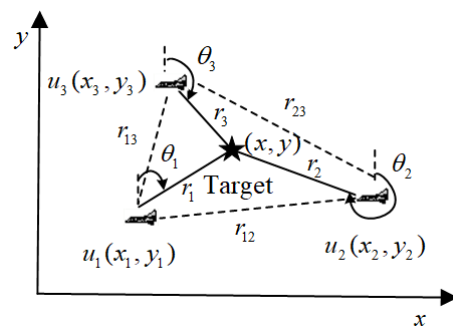


Figure 1. UAV swarm passive localization geometry.

The target bearing angle $\hat{\theta}_k$ measured by the k th UAV consists of the real bearing angle θ_k and the noise n_k .

$$\hat{\theta}_k = \theta_k + n_k \quad (6)$$

where n_k can be modeled by a Gaussian random variable with zero mean and variance σ_{nk}^2 .

3. The Proposed Method

The initial distribution of multiple UAVs are dispersed as illustrated in Figure 2, and each UAV is independently reconnoitering. If a UAV finds the radiation source signal, it will send the bearing information to the UAV within the communication radius. After receiving the radiation source bearing information, the UAVs in the neighborhood adjust their reconnaissance direction.

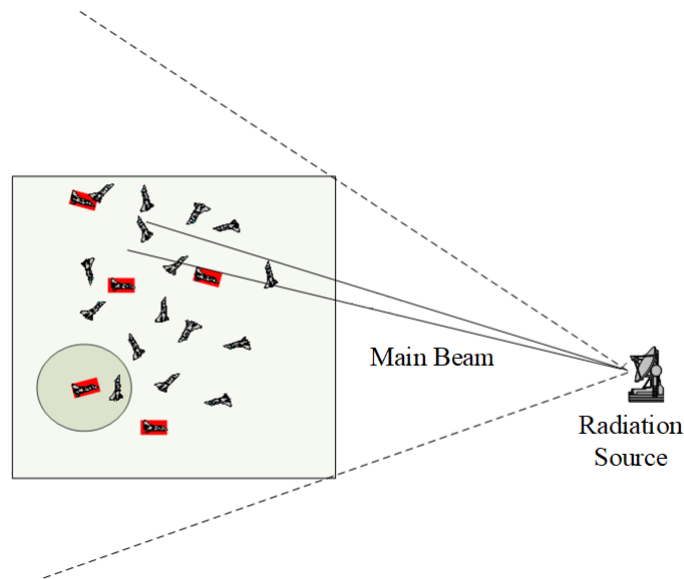


Figure 2. Initial distribution of UAV swarm passive localization.

3.1. Target Initial Position Estimate

As shown in Figure 2, the UAVs marked by the red square indicate that the target was detected at the initial moment. Due to the different directions of the UAV reconnaissance direction, only a small number of UAVs can receive the radiation source signal. These UAVs perform coarse target localization based on the PLE algorithm as the initial estimated position of the target.

The observation equation can be represented as [14]:

$$\mathbf{a}_k \mathbf{p} = \mathbf{b}_k + \boldsymbol{\zeta}_k \quad (7)$$

where $\mathbf{a}_k = [\sin \hat{\theta}_k, -\cos \hat{\theta}_k]$, $\mathbf{b}_k = [\sin \hat{\theta}_k, -\cos \hat{\theta}_k] u_k$, and $\boldsymbol{\zeta}_k = r_k \sin n_k$ is the error term caused by the bearing noise.

From the observation equations of K UAVs, we can obtain

$$\mathbf{A} \mathbf{p} = \mathbf{b} + \boldsymbol{\zeta} \quad (8)$$

where $\mathbf{A} = [\mathbf{a}_1^T \ \mathbf{a}_2^T \ \dots \ \mathbf{a}_K^T]^T$, $\mathbf{b} = [\mathbf{b}_1^T \ \mathbf{b}_2^T \ \dots \ \mathbf{b}_K^T]^T$ and $\boldsymbol{\zeta} = [\boldsymbol{\zeta}_1^T \ \boldsymbol{\zeta}_2^T \ \dots \ \boldsymbol{\zeta}_K^T]^T$. The covariance matrix \mathbf{C} of the noise term $\boldsymbol{\zeta}$ is given by $\mathbf{C} = E[\boldsymbol{\zeta} \boldsymbol{\zeta}^T]$.

According to the principle of LS and (8), the initial estimate position of the target by the PLE algorithm can be expressed as

$$\hat{\mathbf{p}}_0 = (\mathbf{A}^T \mathbf{A})^{-1} \mathbf{A}^T \mathbf{b}. \quad (9)$$

3.2. The Ant Colony Pheromone Mechanism

The ant colony pheromone mechanism is derived from biological phenomena in nature. An ant colony can judge and choose its path using pheromone concentration to improve foraging efficiency. Inspired by ant colony foraging, a passive localization algorithm for UAV swarms based on the ant colony pheromone mechanism is proposed in this section. The ant colony pheromone mechanism can be divided into pheromone injection and pheromone transmission. The pheromone injection mechanism corrects the initial target position estimate based on a single individual, while the pheromone transmission mechanism further improves localization accuracy by weighting and fusing between individuals. The pheromone update mechanism is shown in Algorithm 1.

Algorithm 1 The pheromone update algorithm.

At time t ,
 Step1: Pheromone injection. Each UAV uses the current received target bearing information to correct the initial position estimate \hat{p}_0 .
 1:for $i = 1 : K$
 2: if the i th UAV contains target position information
 3: $\hat{p}_i(t+1) = MLE(\hat{p}_i(t), \hat{\theta}_i(t), u_i)$
 6: End
 7:End
 Step2: Pheromone transmission. Each UAV is weighted by the pheromone transmitted by other UAVs in the communication radius
 1:for $i = 1 : K$
 2: for $j = 1 : K$
 3: if $r_{ij}(k) \leq r_c, (\forall i \neq j)$, and the j th UAV does not contain the target position pheromone
 4: $\hat{p}_j(t+1) = \hat{p}_i(t)$
 5: else if the j th UAV contains the target position pheromone
 6: $\hat{p}_j(t+1) = \omega_{k,1}\hat{p}_i(t) + \omega_{k,2}\hat{p}_j(t)$
 7: End
 8: End
 9:End

In Algorithm 1, $\hat{p}_i(t)$ and $\hat{p}_j(t)$ represent the existing target position estimate of the i th UAV and the j th UAV, respectively. $\hat{p}_i(t+1)$ and $\hat{p}_j(t+1)$ represent the target position estimate of the i th UAV and the j th UAV at the next moment, respectively. $MLE(\hat{p}_i(t), \hat{\theta}_i(t), u_i)$ denotes the MLE iteration algorithm, which uses the gradient descent method and the bearing information received by the i th UAV $\hat{\theta}_i(t)$ to correct $\hat{p}_i(t)$. $\omega_{k,1}$ and $\omega_{k,2}$ correspond to the weight information of different UAV pheromones, respectively.

3.2.1. Pheromone Injection

In the pheromone injection mechanism, each UAV uses the MLE algorithm and the current observed bearing information to correct the coarse target position estimate. The MLE of the target position is defined as the value of \mathbf{p} that maximizes the likelihood function. The likelihood function of the target bearing measured by K UAVs can be expressed as [40]:

$$f(\hat{\boldsymbol{\theta}}|\mathbf{p}) = \frac{1}{(2\pi)^{K/2}|\mathbf{Q}|^{1/2}} e^{-1/2(\hat{\boldsymbol{\theta}}-\boldsymbol{\theta}(\mathbf{p}))^T\mathbf{Q}^{-1}(\hat{\boldsymbol{\theta}}-\boldsymbol{\theta}(\mathbf{p}))} \quad (10)$$

where $\mathbf{Q} = \text{diag}(\sigma_{n1}^2, \sigma_{n2}^2, \dots, \sigma_{nK}^2)$ is the covariance matrix of bearing noise; $\text{diag}()$ represents the function that transforms the row vector into a diagonal matrix. $\boldsymbol{\theta}(\mathbf{p}) = [\theta_1(p) \theta_2(p) \dots \theta_K(p)]^T$ is the true bearing vector and $\hat{\boldsymbol{\theta}} = [\hat{\theta}_1 \hat{\theta}_2 \dots \hat{\theta}_K]^T$ is the measured history bearings of the k th UAV.

The maximum value of the likelihood function can also be expressed as the minimum value of the cost function:

$$\min f(\mathbf{p}) = (\hat{\boldsymbol{\theta}} - \boldsymbol{\theta}(\mathbf{p}))^T \mathbf{Q}^{-1} (\hat{\boldsymbol{\theta}} - \boldsymbol{\theta}(\mathbf{p})). \quad (11)$$

The initial estimated position of the target obtained by Equation (9) is used as the input of the likelihood function, and the gradient descent method is used to iterate the target position. The estimated position of the target update is given by:

$$\hat{\mathbf{p}}_{new} = \hat{\mathbf{p}}_{old} - \alpha \left[\frac{\partial f(\mathbf{p})}{\partial x} \quad \frac{\partial f(\mathbf{p})}{\partial y} \right]^T \quad (12)$$

where $\hat{\mathbf{p}}_{new}$ and $\hat{\mathbf{p}}_{old}$ represent the target position before and after the update, respectively. α is the learning rate of the MLE algorithm. In the above, $\frac{\partial f(\mathbf{p})}{\partial x}$ and $\frac{\partial f(\mathbf{p})}{\partial y}$ are the partial derivatives of the function with respect to the target position [40], which are given by:

$$\frac{\partial f(\mathbf{p})}{\partial x} = 2(\theta(\mathbf{p}) - \hat{\rho})^T \mathbf{Q}^{-1} \frac{\partial \theta(\mathbf{p})}{\partial x}, \tag{13}$$

$$\frac{\partial f(\mathbf{p})}{\partial y} = 2(\theta(\mathbf{p}) - \hat{\rho})^T \mathbf{Q}^{-1} \frac{\partial \theta(\mathbf{p})}{\partial y}. \tag{14}$$

where $\frac{\partial \theta(\mathbf{p})}{\partial x}$ and $\frac{\partial \theta(\mathbf{p})}{\partial y}$ can be obtained by:

$$\frac{\partial \theta(\mathbf{p})}{\partial x} = \left[\frac{-\Delta y_1}{r_1^2} \quad \frac{-\Delta y_2}{r_2^2} \quad \dots \quad \frac{-\Delta y_K}{r_K^2} \right]^T, \tag{15}$$

$$\frac{\partial \theta(\mathbf{p})}{\partial y} = \left[\frac{-\Delta x_1}{r_1^2} \quad \frac{-\Delta x_2}{r_2^2} \quad \dots \quad \frac{-\Delta x_K}{r_K^2} \right]^T. \tag{16}$$

Here, $\Delta y_k = y - y_k$, $\Delta x_k = x - x_k$.

3.2.2. Pheromone Transmission

As shown in Figure 3, each UAV also receives the pheromone transmitted by other UAVs in the communication range when performing pheromone transmission. Compared with the initial state in Figure 2, more UAVs will be added to locate the radiation source through the pheromone transmission mechanism. If the current UAV already contains the target position estimate, it is fused with those estimates obtained by the UAVs within the communication radius in the Bayesian manner. After a limited number of communications and updates, each UAV receives the most accurate and consistent target bearing information.

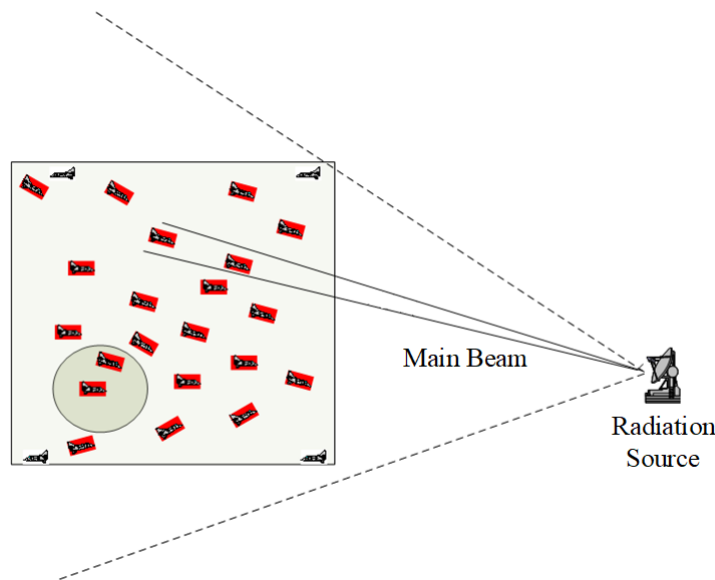


Figure 3. Distribution of UAV swarm passive localization after pheromone transmission.

When the bearing noise n_k is small, ξ_k can be similarly expressed as:

$$\xi_k = r_k \sin n_k \approx r_k n_k. \tag{17}$$

The covariance matrix of noise term ξ can be obtained by:

$$\mathbf{C} = \text{diag}(r_1^2 \sigma_{n1}^2, r_2^2 \sigma_{n2}^2, \dots, r_k^2 \sigma_{nk}^2). \tag{18}$$

The weighted matrix \mathbf{W} is given by:

$$\mathbf{W} = \mathbf{C}^{-1} = \text{diag}(1/(r_1^2\sigma_{n1}^2), 1/(r_2^2\sigma_{n2}^2), \dots, 1/(r_k^2\sigma_{nk}^2)). \quad (19)$$

In the case of K UAVs, the weight of m th UAV is given by:

$$\omega_{k,m} = \frac{1/(r_m^2\sigma_{nm}^2)}{\sum_{i=1}^K (1/(r_i^2\sigma_{ni}^2))}. \quad (20)$$

Assuming that the estimated value $\hat{\mathbf{p}}$ has a linear relationship with the measured values $\hat{\mathbf{p}}_{k,1}, \hat{\mathbf{p}}_{k,2}, \dots, \hat{\mathbf{p}}_{k,K}$ [41], the estimate value of multi-UAVs can be expressed as:

$$\hat{\mathbf{p}} = \omega_{k,1}\hat{\mathbf{p}}_{k,1} + \omega_{k,2}\hat{\mathbf{p}}_{k,2} + \dots + \omega_{k,K}\hat{\mathbf{p}}_{k,K}. \quad (21)$$

Combining Equations (20) and (21), the position estimation of the target can be represented as:

$$\hat{\mathbf{p}} = \frac{1/(r_1^2\sigma_{n1}^2)\hat{\mathbf{p}}_{k,1} + 1/(r_2^2\sigma_{n2}^2)\hat{\mathbf{p}}_{k,2} + \dots + 1/(r_K^2\sigma_{nK}^2)\hat{\mathbf{p}}_{k,K}}{\sum_{i=1}^K (1/(r_i^2\sigma_{ni}^2))}. \quad (22)$$

In the unbiased estimation problem, the Cramer–Rao lower bound (CRLB) is usually used to measure the validity of the estimate value. The closer the root mean square error (RMSE) of an estimate is to CRLB, the more accurate the estimate is. To calculate CRLB, the Fisher Matrix is introduced as follows:

$$\mathbf{F} = \begin{bmatrix} -\mathbb{E}\left[\frac{\partial^2}{\partial x^2} f(\hat{\boldsymbol{\theta}} | \mathbf{p})\right] & -\mathbb{E}\left[\frac{\partial^2}{\partial x \partial y} f(\hat{\boldsymbol{\theta}} | \mathbf{p})\right] \\ -\mathbb{E}\left[\frac{\partial^2}{\partial y \partial x} f(\hat{\boldsymbol{\theta}} | \mathbf{p})\right] & -\mathbb{E}\left[\frac{\partial^2}{\partial y^2} f(\hat{\boldsymbol{\theta}} | \mathbf{p})\right] \end{bmatrix} \quad (23)$$

$$\mathbf{F} = \left[\frac{\partial \boldsymbol{\theta}(\mathbf{p})}{\partial x} \quad \frac{\partial \boldsymbol{\theta}(\mathbf{p})}{\partial y} \right]^T \mathbf{Q}^{-1} \left[\frac{\partial \boldsymbol{\theta}(\mathbf{p})}{\partial x} \quad \frac{\partial \boldsymbol{\theta}(\mathbf{p})}{\partial y} \right] \quad (24)$$

\mathbf{Q} is the initial value of the covariance matrix \mathbf{C} of the noise term $\boldsymbol{\zeta}$.

$$\mathbf{Q} = \text{diag}(\sigma_{n1}^2, \sigma_{n2}^2, \dots, \sigma_{nK}^2). \quad (25)$$

Combining with Equations (15) and (16), the Fisher matrix can be represented as

$$\mathbf{F} = \sum_{k=1}^K \frac{1}{\sigma_{nK}^2 r_k^4} \begin{bmatrix} (\Delta y_K)^2 & -\Delta x_K \Delta y_K \\ -\Delta x_K \Delta y_K & (\Delta x_K)^2 \end{bmatrix}. \quad (26)$$

The CRLB is equal to the inverse of the Fisher matrix:

$$\text{CRLB} = \mathbf{F}^{-1}. \quad (27)$$

To summarize the proposed algorithm (Figure 4):

- (a) A small number of UAVs receiving radiation source signals use PLE to compute an initial target location estimate $\hat{\mathbf{p}}_0$;
- (b) Based on the pheromone injection mechanism, each UAV uses MLE to self-correct to obtain the next moment estimate $\hat{\mathbf{p}}_i(t+1)$;
- (c) Radiation source information can be transmitted to the whole network through the pheromone transmission mechanism. Each UAV is weighted with other individuals within the communication radius to obtain the revised target location estimate $\hat{\mathbf{p}}_j(t+1)$.

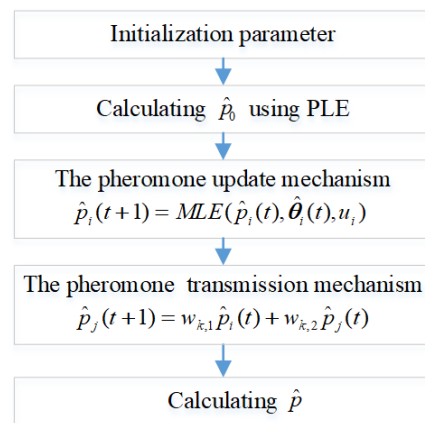


Figure 4. The flowchart of the proposed algorithm.

4. Simulation Results

In order to verify the performance of the proposed method, we present two numerical examples in this section. One is the case of a single-fixed target and the other is the case of a single-unfixed target. The proposed method is compared to the PLE, MLE, and weighted pseudo-linear estimator (WPLE) [14] algorithms. In the above algorithms, the MLE is computed using the gradient descent iterations and the initial estimation of the target position is set to be the result of the PLE. In the proposed method, the initial target position estimate is obtained by a small number of UAVs based on the PLE algorithm. Then, the ant colony pheromone mechanism is introduced to correct the initial target position. In the simulation experiment, the bearing measurement errors are assumed to be independent and identically distributed zero-mean Gaussian random variables.

4.1. A Single-Fixed Target

The simulation scenario is shown in Figure 5. The true target location is placed at $(-155, 175)$ m. 20 UAVs are randomly distributed in an area of $200 \text{ m} \times 200 \text{ m}$. The range of bearing noise standard deviation σ_{nk} is set from 1° to 8° , corresponding to 0.0175 to 0.1396 rad.

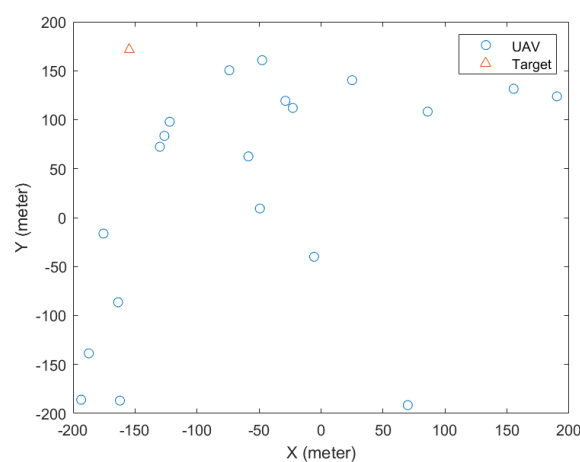


Figure 5. The simulation scenario of a single-fixed target.

4.1.1. Bearing Standard Deviation

The RMSEs of the position estimate with the standard deviation of the bearing measurement noise ranging from 0.0175 to 0.1396 rad are shown in Figure 6. The communication radius of the UAVs r_c is set to 60 m. Figure 6 demonstrates the superior performance of the proposed method compared with the PLE algorithm. The proposed method, MLE,

and WPLE are very close to the CRLB for small measurement noise. The bias of position estimate is illustrated in Figure 7. We observe that the bias curves of the MLE and the proposed method are relatively close, and their performance is better than the PLE and the WPLE algorithms. From Figures 6 and 7, it can be seen that the localization performance of the proposed method is very close to the MLE algorithm. The maximum RMSE difference between the proposed method and MLE algorithm does not exceed 0.3 m. Compared with the MLE algorithm, the proposed method only uses the local observation information of UAVs. The advantage of the proposed method is in realizing the distributed processing of UAV local observation information under limited communication and observation range.

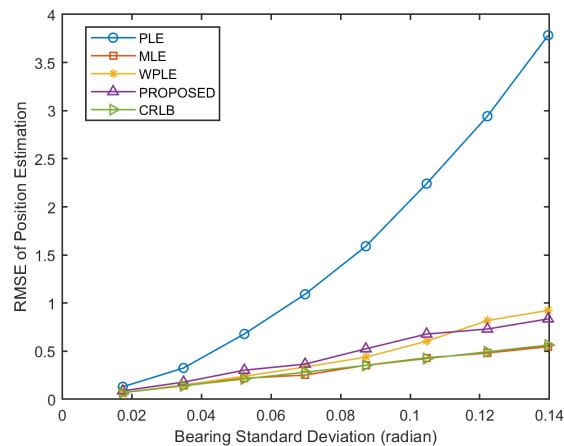


Figure 6. RMSE of position estimation versus bearing standard deviation.

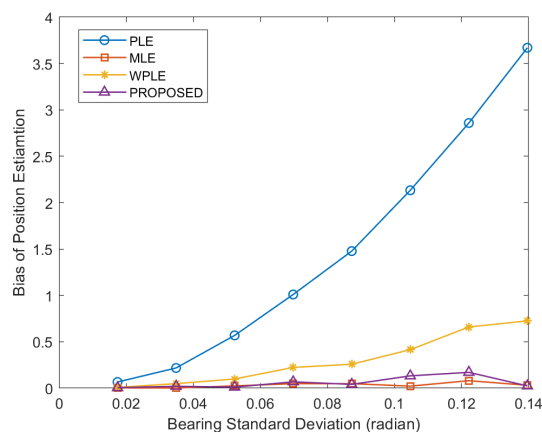


Figure 7. Bias of position estimation versus bearing standard deviation.

4.1.2. The Number of UAVs

The RMSEs of the position estimate as a function of the number of UAVs ranging from 30 to 50 are shown in Figure 8. The bearing noise standard deviation σ_{nk} and the UAV's communication radius r_c are set to $4\pi/180$ rad and 60 m, respectively. It can be seen that the performance of the proposed method is better than the PLE and the WPLE. The performance of the MLE method is closed to the CRLB. The bias of the PLE, WPLE, and MLE are compared with the proposed method in Figure 9. The proposed method produces smaller bias than that of the PLE, WPLE, and MLE over the measurement noise examined.

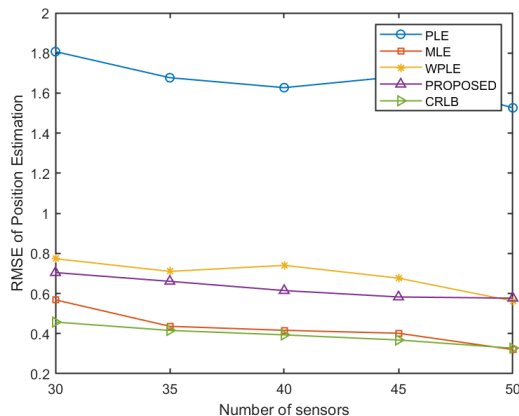


Figure 8. RMSE of position estimation versus bearing standard deviation.

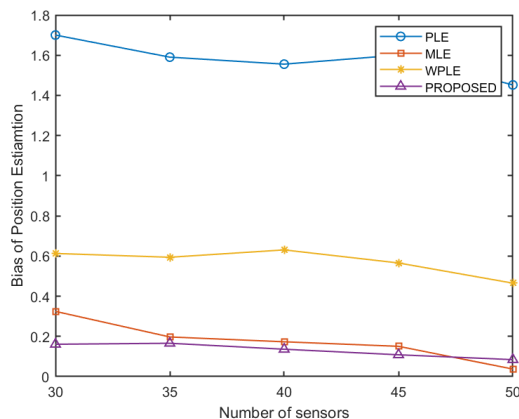


Figure 9. Bias of position estimation versus bearing standard deviation.

4.1.3. The Communication Radius of UAV

Figures 10 and 11 illustrate the RMSE and bias results for the UAV’s communication radius ranging from 10 m to 100 m, respectively. The bearing noise standard deviation σ_{nk} is set to $4\pi/180$ rad. As expected, with the increase of the communication radius of the UAVs, more UAVs are weighted in the pheromone transmission mechanism; therefore, the RMSE and bias of the proposed method gradually decrease.

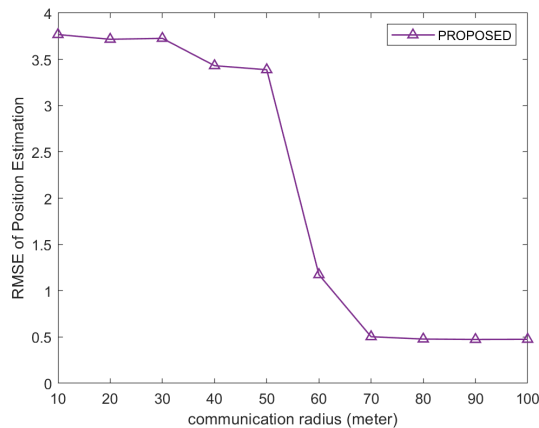


Figure 10. RMSE of position estimation versus communication radius.

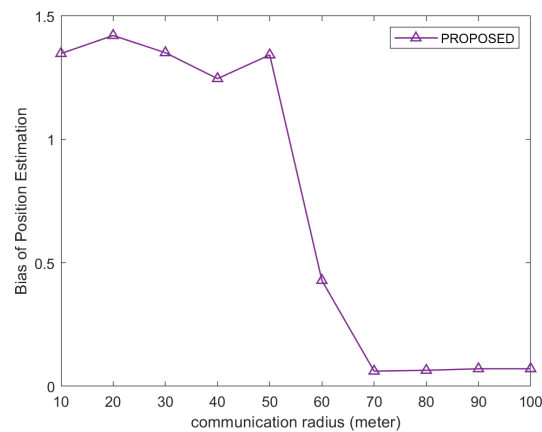


Figure 11. Bias of position estimation versus communication radius.

4.2. A Single-Unfixed Target

A single-unfixed target localization geometry employed in the RMSE and bias is depicted in Figure 12. The target follows a linear trajectory defined by $y = x$ and generates $N = 5$ target positions with equal intervals. The bearing noise standard deviation σ_{nk} and the UAVs' communication radius r_c are set to $4\pi/180$ rad and 60 m, respectively. The number of UAVs is set to 20.

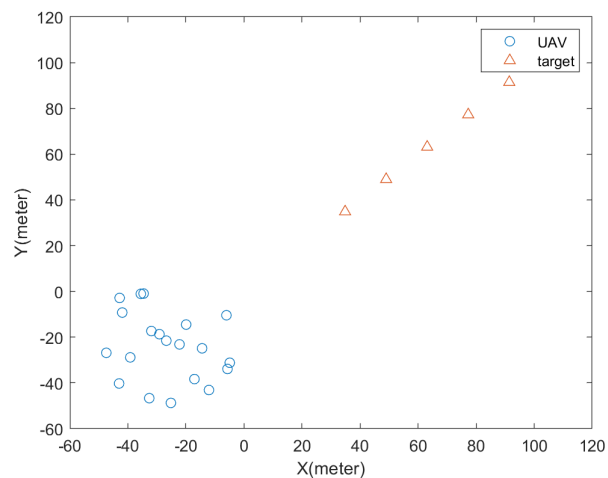


Figure 12. The simulation scenario of a single-unfixed target.

The RMSE and the bias of position estimate versus the target distance are shown in Figures 13 and 14, respectively. Since the UAVs are gathered on one side of the target, the traditional distributed fusion method obtains relatively little target bearing information. However, the proposed method can realize the sharing of local localization information through the pheromone transmission mechanism, and so can achieve consistency of global estimation information. Each UAV is weighted with other UAVs in the neighborhood to improve positioning accuracy. The performance of the proposed method is better than the PLE, MLE, and WPLE algorithms. The RMSE curves of the PLE, MLE, and WPLE are close to each other. The position estimation bias results show that the proposed method yields the smallest bias. The PLE algorithm exhibits the worst bias among all the algorithms. While the biases of the MLE and WPLE algorithms are not as small as that of the proposed method, their errors are closer to the PLE algorithm.

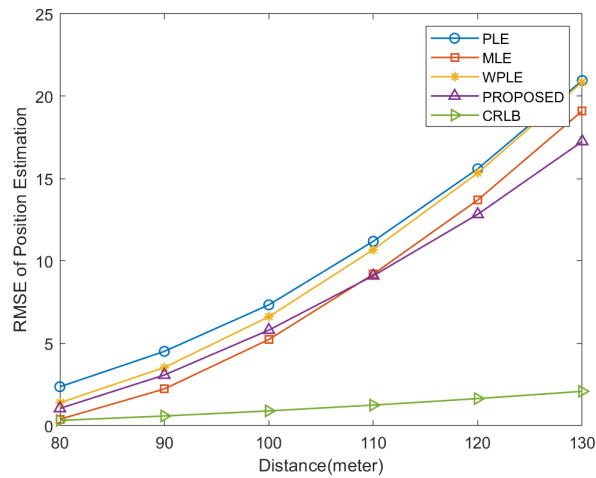


Figure 13. RMSE of position estimation versus target distance.

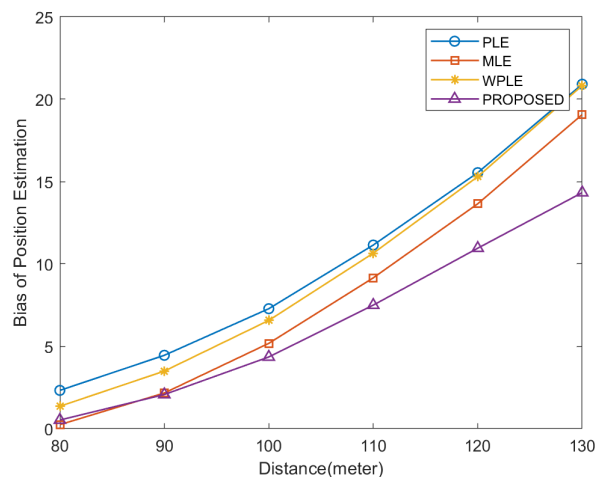


Figure 14. Bias of position estimation versus target distance.

5. Conclusions

In order to solve the problem of passive localization of UAV swarms under limited communication and observation range, a passive localization algorithm based on the ant colony pheromone mechanism was proposed in this paper. Firstly, the initial target position estimate was calculated by a small number of UAVs based on the PLE algorithm. Then, an ant colony pheromone mechanism, which includes pheromone injection and pheromone transmission, was introduced to improve the localization accuracy. Pheromone injection was used to modify the initial target localization estimate of a single individual. The information interaction between UAV individuals was used to improve the localization accuracy in the pheromone transmission mechanism. Finally, the localization performances of different algorithms and parameters were compared in simulation. The experimental results shown that the system with the added ant colony pheromone mechanism has higher localization correctness and RMSE performance close to the CRLB for small noise.

Author Contributions: Conceptualization, Y.Z.; methodology, Y.Z. and D.S.; software, Y.Z. and B.D.; validation, Y.Z.; formal analysis, Y.Z.; investigation, Y.Z.; resources, B.R.; data curation, M.S.; writing—original draft preparation, Y.Z.; writing—review and editing, Y.Z.; visualization, B.R.; supervision, W.W.; project administration, W.W.; funding acquisition, Y.Z. and D.S. All authors have read and agreed to the published version of the manuscript.

Funding: This research was funded by the National Science Foundation for Young Scientists of China under Grant 62101558, the Intelligent Innovation Foundation under Grant 201-CXCY-A01-08-19-02, and the Research Foundation of National University of Defense University under Grant Zk21-38.

Data Availability Statement: Not applicable.

Conflicts of Interest: The authors declare no conflict of interest.

Abbreviations

The following abbreviations are used in this manuscript:

UAV	Unmanned aerial vehicle
PLE	Pseudo linear estimation
ML	Maximum likelihood
CRLB	Cramer-Rao lower bound
TDOA	Time difference of arrival
RSS	Received signal strength
FDOA	Frequency difference of arrival
AOA	Angle of arrival
LS	Least square
DWLS	Distance weighted least squares
NLOS	Non-line of sight
RMSE	Root mean square error

References

- Zhou, Y.; Rao, B.; Wang, W. UAV Swarm Intelligence: Recent Advances and Future Trends. *IEEE Access* **2020**, *8*, 183856–183878. [[CrossRef](#)]
- Cheung, K.W.; So, H.C. A multidimensional scaling framework for mobile location using time-of-arrival measurements. *IEEE Trans. Signal Process.* **2005**, *53*, 460–470. [[CrossRef](#)]
- Yan, Y.; Wang, H.; Shen, X.; He, K.; Zhong, X. TDOA-based source collaborative localization via semidefinite relaxation in sensor networks. *Int. J. Distrib. Sens. Netw.* **2015**, *11*, 248970. [[CrossRef](#)]
- Nguyen, N.H.; Doğançay, K. Optimal geometry analysis for multistatic TOA localization. *IEEE Trans. Signal Process.* **2016**, *64*, 4180–4193. [[CrossRef](#)]
- Salari, S.; Chan, F.; Chan, Y.T.; Read, W. TDOA estimation with compressive sensing measurements and Hadamard matrix. *IEEE Trans. Aerosp. Electron. Syst.* **2018**, *54*, 3137–3142. [[CrossRef](#)]
- Xiong, W.; Schindelbauer, C.; So, H.C.; Liang, J.; Wang, Z. A neurodynamic optimization approach to TDOA-based IoT localization in NLOS environments. *arXiv* **2020**, arXiv:2009.06281.
- Ouyang, R.W.; Wong, A.K.S.; Lea, C.T. Received signal strength based wireless localization via semidefinite programming: Noncooperative and cooperative schemes. *IEEE Trans. Veh. Technol.* **2010**, *59*, 1307–1318. [[CrossRef](#)]
- Coluccia, A.; Ricciato, F. On ML estimation for automatic RSS-based indoor localization. In Proceedings of the IEEE 5th International Symposium on Wireless Pervasive Computing 2010, Modena, Italy, 5–7 May 2010; IEEE: Piscataway, NJ, USA, 2010; pp. 495–502.
- Lin, L.; So, H.C.; Chan, Y.T. Accurate and simple source localization using differential received signal strength. *Digit. Signal Process.* **2013**, *23*, 736–743. [[CrossRef](#)]
- Hu, Y.; Leus, G. Robust differential received signal strength-based localization. *IEEE Trans. Signal Process.* **2017**, *65*, 3261–3276. [[CrossRef](#)]
- Ketabalian, H.; Biguesh, M.; Sheikhi, A. A closed-form solution for localization based on RSS. *IEEE Trans. Aerosp. Electron. Syst.* **2019**, *56*, 912–923. [[CrossRef](#)]
- Amar, A.; Leus, G.; Friedlander, B. Emitter localization given time delay and frequency shift measurements. *IEEE Trans. Aerosp. Electron. Syst.* **2012**, *48*, 1826–1837. [[CrossRef](#)]
- Lingren, A.G.; Gong, K.F. Position and velocity estimation via bearing observations. *IEEE Trans. Aerosp. Electron. Syst.* **1978**, *4*, 564–577. [[CrossRef](#)]
- Doğançay, K. Bearings-only target localization using total least squares. *Signal Process.* **2005**, *85*, 1695–1710. [[CrossRef](#)]
- Son, B.K.; An D.J.; Lee, J.H. Performance analysis of AOA-Based localization using the LS approach: Explicit expression of mean-squared error. *J. Sens.* **2020**, *11*, 1–22. [[CrossRef](#)]
- Gavish, M.; Weiss, A.J. Performance analysis of bearing-only target location algorithms. *IEEE Trans. Aerosp. Electron. Syst.* **1992**, *28*, 817–828. [[CrossRef](#)]
- Wang, Z.; Luo, J.A.; Zhang, X.P. A novel location penalized maximum likelihood estimator for bearing-only target localization. *IEEE Trans. Signal Process.* **2012**, *60*, 6166–6181. [[CrossRef](#)]

18. Rui, L.; Ho, K.C. Bias analysis of source localization using the maximum likelihood estimator. In Proceedings of the 2012 IEEE International Conference on Acoustics, Speech and Signal Processing (ICASSP), Kyoto, Japan, 25–30 March 2012; IEEE: Piscataway, NJ, USA, 2012; pp. 2605–2608.
19. Xu, J.; Ma, M.; Law, C.L. AOA cooperative position localization. In Proceedings of the IEEE GLOBECOM 2008—2008 IEEE Global Telecommunications Conference, New Orleans, LA, USA, 30 November–4 December 2008; IEEE: Piscataway, NJ, USA, 2008; pp. 1–5.
20. Wang, W.; Bai, P.; Zhou, Y.; Liang, X.; Wang, Y. Optimal configuration analysis of AOA localization and optimal heading angles generation method for UAV swarms. *IEEE Access* **2019**, *7*, 70117–70129. [[CrossRef](#)]
21. Wan, P.; Huang, Q.; Lu, G.; Wang, J.; Yan, Q.; Chen, Y. Passive localization of signal source based on UAVs in complex environment. *China Commun.* **2020**, *17*, 107–116. [[CrossRef](#)]
22. Wang, Y.; Ho, K.C. An asymptotically efficient estimator in closed-form for 3D AOA localization using a sensor network. *IEEE Trans. Wirel. Commun.* **2015**, *14*, 6524–6535. [[CrossRef](#)]
23. Luo, J.A.; Zhang, X.P.; Wang, Z. A new passive source localization method using AOA-GROA-TDOA in wireless sensor array networks and its Cramér-Rao bound analysis. In Proceedings of the 2013 IEEE International Conference on Acoustics, Speech and Signal Processing, Vancouver, BC, Canada, 26–31 May 2013; IEEE: Piscataway, NJ, USA, 2013; pp. 4031–4035.
24. Luo, J.A.; Tan, Z.W.; Peng, D.L. A novel bearing-assisted TDOA-GROA approach for passive source localization. *Int. J. Intell. Comput. Cybern.* **2018**, *11*, 2–19. [[CrossRef](#)]
25. Werner, J.; Wang, J.; Hakkarainen, A.; Cabric, D.; Valkama, M. Performance and Cramer Rao bounds for DoA/RSS estimation and transmitter localization using sectorized antennas. *IEEE Trans. Veh. Technol.* **2015**, *65*, 3255–3270. [[CrossRef](#)]
26. Tomic, S.; Beko, M.; Dinis, R. Distributed RSS-AoA based localization with unknown transmit powers. *IEEE Wirel. Commun. Lett.* **2015**, *5*, 392–395. [[CrossRef](#)]
27. Ho, K.C.; Lu, X.; Kovavisaruch, L. Source localization using TDOA and FDOA measurements in the presence of receiver location errors: Analysis and solution. *IEEE Trans. Signal Process.* **2007**, *55*, 684–696. [[CrossRef](#)]
28. Noroozi, A.; Oveis, A.H.; Hosseini, S.M.; Sebt, M.A. Improved algebraic solution for source localization from TDOA and FDOA measurements. *IEEE Wirel. Commun. Lett.* **2017**, *7*, 352–355. [[CrossRef](#)]
29. Dexiu, H.U.; Huang, Z.; Zhang, S.; Jianhua, L.U. Joint TDOA, FDOA and differential doppler rate estimation: Method and its performance analysis. *Chin. J. Aeronaut.* **2018**, *31*, 137–147.
30. Zhang, X.; Wang, F.; Li, H.; Hamed, B. Maximum likelihood and IRLS based moving source localization with distributed sensors. *IEEE Trans. Aerosp. Electron. Syst.* **2020**, *57*, 448–461. [[CrossRef](#)]
31. Aernouts, M.; BriLam, N.; Berkvens, R.; Weyn, M. TDAoA: A combination of TDoA and AoA localization with LoRa WAN. *Internet Things* **2020**, *11*, 100–236. [[CrossRef](#)]
32. Vidal-Valladares, M.G.; Díaz, M.A. A Femto-Satellite Localization Method Based on TDOA and AOA Using Two CubeSats. *Remote Sens.* **2022**, *14*, 1101. [[CrossRef](#)]
33. Luo, J.A.; Wang, Z. A novel closed-form estimator for 3D source localization using angle of arrivals and gain ratio of arrivals. In Proceedings of the 2017 36th Chinese Control Conference (CCC), Dalian, China, 26–28 July 2017; IEEE: Piscataway, NJ, USA, 2017; pp. 5179–5182.
34. Baggio, A.; Langendoen, K. Monte Carlo localization for mobile wireless sensor networks. *Ad Hoc Netw.* **2008**, *6*, 718–733. [[CrossRef](#)]
35. Pathirana, P.N.; Bulusu, N.; Savkin, A.V.; Jha, S. Node localization using mobile robots in delay-tolerant sensor networks. *IEEE Trans. Mob. Comput.* **2005**, *4*, 285–296. [[CrossRef](#)]
36. Dong, L. Cooperative localization and tracking of mobile ad hoc networks. *IEEE Trans. Signal Process.* **2012**, *60*, 3907–3913. [[CrossRef](#)]
37. Coloni, A.; Dorigo, M.; Maniezzo, V. Distributed optimization by ant colonies. In Proceedings of the First European Conference on Artificial Life, Paris, France, 11–13 December 1991; Volume 142, pp. 134–142.
38. Guntsch, M.; Middendorf, M. Pheromone Modification Strategies for Ant Algorithms Applied to Dynamic TSP. In Proceedings of the Workshops on Applications of Evolutionary Computation, Como, Italy, 18–20 April 2001; Springer: Berlin/Heidelberg, Germany, 2001; pp. 213–222.
39. Luo, J.A.; Shao, X.H.; Peng, D.L.; Zhang, X.P. A novel subspace approach for bearing-only target localization. *IEEE Sens. J.* **2019**, *99*, 8174–8182. [[CrossRef](#)]
40. Wang, W.; Marelli, D.; Fu, M. Multiple-vehicle localization using maximum likelihood Kalman filtering and ultra-wideband signals. *IEEE Sens. J.* **2020**, *21*, 4949–4956. [[CrossRef](#)]
41. Kay, S.M. *Fundamentals of Statistical Signal Processing: Estimation Theory*; Prentice-Hall, Inc.: Hoboken, NJ, USA, 1993.